ACCSCIENCE PUBLISHING

Eurasian Journal of Medicine and Oncology

ORIGINAL RESEARCH ARTICLE

Liquid biopsy-based longitudinal monitoring of copy number variations in six biomarker genes reveals exploratory associations with disease progression and treatment resistance in localized soft tissue sarcomas

Aneta Borkowska[1†*], Teresa Szczepińska[2†], Michał Sitek[2], Wiktoria Trynkos[2], Izabela Ziuzia-Graczyk[2], Anna Staniszewska[3], Łukasz Kuryk[1,4], Deepak Kala[5], Ewelina Holm Bidstrup[2], Piotr Rutkowski[1], and Monika Staniszewska[2*]

[1]Department of Soft Tissue, Bone Sarcoma and Melanoma, Maria Sklodowska-Curie National Research Institute of Oncology, Warsaw, Masovia, Poland

[2]Centre for Advanced Materials and Technologies CEZAMAT, Warsaw University of Technology, Warsaw, Masovia, Poland

[3]Central Clinical Hospital, Medical University of Warsaw, Warsaw, Masovia, Poland

[4]National Institute of Public Health-National Institute of Hygiene, Warsaw, Masovia, Poland

[5]Centera Tetrahertz Laboratory, Institute of High-Pressure Physics, Polish Academy of Sciences, Warsaw, Masovia, Poland

[†]*These authors contributed equally to this work.*

***Corresponding authors:**
Aneta Borkowska (aneta.borkowska@nio.gov.pl);
Monika Staniszewska (monika.staniszewska@pw.edu.pl)

Citation: Borkowska A, Szczepińska T, Sitek M, *et al*. Liquid biopsy-based longitudinal monitoring of copy number variations in six biomarker genes reveals exploratory associations with disease progression and treatment resistance in localized soft tissue sarcomas. *Eurasian J Med Oncol*. doi: 10.36922/EJMO026260300

Received: June 22, 2026

Revised: August 2, 2026

Accepted: September 4, 2026

Published online: November 16, 2026

Copyright: © 2026 Author(s). This is an Open-Access article distributed under the terms of the Creative Commons Attribution License, permitting distribution, and reproduction in any medium, provided the original work is properly cited.

Publisher's Note: AccScience Publishing remains neutral with regard to jurisdictional claims in published maps and institutional affiliations.

Abstract

Introduction: Soft tissue sarcomas (STS) are rare cancers without validated biomarkers for monitoring or prognosis. Liquid biopsy (LB) enables minimally invasive tumor tracking.

Objectives: This study aims to identify prognostic biomarkers in STS by assessing whether copy number variations (CNVs) of key genes correlate with outcomes, enabling early risk stratification and monitoring.

Methods: We conducted a preliminary longitudinal CNV analysis in plasma cell-free DNA from 19 patients using droplet digital polymerase chain reaction, measuring CNVs at multiple treatment stages (B1–B6). Statistical analyses were performed in R (v.4.4.3). Continuous variables are shown as median (interquartile range), and categorical variables as counts (%). Benjamini–Hochberg adjustment was applied, and progression-free survival (PFS) was analyzed using Kaplan–Meier and the log-rank test.

Results: Associations between CNVs and tumor size, necrosis, treatment response, disease progression, and PFS were observed. B1–B4 showed interconnected CNVs, involving *TP53*, *RB1*, *MDM2*, *BRAF*, *MET*, and *HSP90*. Progression may be associated with elevated CNVs for *MDM2* and *MET* during chemotherapy (B2), and for *TP53*, *RB1*, *MDM2*, and *HSP90* following radiotherapy (B3). At baseline, *MDM2* CNV was higher in non-responders and increased during therapy in patients who subsequently experienced progression, which may be associated with poorer response to chemotherapy and radiotherapy. A *p*-value minimization framework suggested gene-specific CNV thresholds at B2 and B3, with higher CNV linked to shorter PFS.

Conclusion: Longitudinal LB profiling indicates that genomic changes in STS are linked to outcomes and resistance. *MDM2* emerged as a potential biomarker. Given

the small, exploratory study cohort, these findings need cautious interpretation and validation in larger groups.

Keywords: Soft tissue sarcoma; Liquid biopsy; Biomarkers; Progression; Copy number variations; Progression-free survival

1. Introduction

Soft tissue sarcomas (STS) are a rare group of over 100 diverse cancers, which hampers the development of new diagnostic and therapeutic tools due to challenges in conducting subtype-specific studies and the slow pace of identifying reliable biomarkers.[1,2] A key technology that facilitates their analysis is liquid biopsy (LB), which enables repeated sampling of blood or other body fluids to capture dynamic changes in tumor biology.[1,3] LB has already been used to support screening, early relapse detection, and personalized treatment, highlighting its potential relevance for STS.[4,5] However, research on LB in sarcomas remains in its early stages and has primarily focused on cell- free DNA (cfDNA), circulating tumor DNA (ctDNA), microRNA (miRNA), and proteomic and metabolic markers.[1,4,6] Several analytical approaches have been developed for the detection and characterization of cfDNA and ctDNA, including polymerase chain reaction (PCR)-based techniques (e.g., quantitative PCR and digital droplet PCR) and next-generation sequencing (NGS).[1,7] While many customized assays have demonstrated high specificity (over 95%) in cancer patients, such as CancerSEEK (PCR)[8] and CAPPseq (NGS)[9], their sensitivities can vary significantly depending on the technology and tumor type.[8,10-12] Although methods such as CAPPseq have shown promising sensitivity and specificity in small cohorts of leiomyosarcoma patients, these preliminary findings are insufficient for broad clinical adoption across the diverse spectrum of STS.[9] Braig *et al.*[13] demonstrated that plasma cfDNA concentrations are elevated in STS patients with active disease compared with healthy individuals and patients in remission, indicating that cfDNA levels alone may serve as a marker for detecting disease recurrence.[14] None of the currently available prognostic tools for STS incorporates serum biomarkers, molecular alterations, genomic profiling, or radiomic features as predictive variables.[15] The American Joint Committee on Cancer/ Union for International Cancer Control (AJCC/UICC) staging system primarily considered tumor grade, size, depth, lymph node involvement, and distant metastases, but overlooked tumor location and histologic subtype.[16] To enhance prognostic accuracy, several nomograms have been developed since 2005 to predict the risk of local recurrence, overall survival, and distant metastases.[17-20] The integration of serum markers has already been shown to improve the performance of existing nomograms, highlighting the potential value of multimodal approaches.[21,22] The integration of molecular and genomic data into prognostic models represents a critical future direction in STS.[17-20] In this context, copy number variation (CNV) analysis, particularly the assessment of *TP53, MDM2, RB1, MET, BRAF,* and *HSP90*, may provide clinically relevant information that complements existing clinicopathological tools and supports improved risk stratification.[17-20] The selected biomarkers were identified through a literature-based approach and have been previously implicated in the pathogenesis, diagnosis, and clinical management of sarcomas.[1,23-35] CNV analysis is a key tool for identifying genomic alterations linked to tumor progression and outcomes. In STS, profiling CNVs in genes such as *TP53*, *MDM2*, and *RB1* can reveal distinct patient subgroups beyond those identified by traditional methods.[36] This study aims to improve risk stratification and clinical management by examining CNVs in these genes, particularly *MDM2* amplification, which is valuable in diagnosing dedifferentiated liposarcoma.[37]

The mouse double minute 2 (*MDM2*) proto-oncogene is among the most promising biomarkers for some subtypes of liposarcoma.[1,37] In addition to its diagnostic capabilities, elevated *MDM2* levels, particularly when measured in extracellular vesicles, can differentiate liposarcoma patients from healthy individuals and tend to decrease after tumor removal.[1,23,24] An increase in *MDM2* levels following surgery is associated with recurrence of the disease, highlighting its potential for early detection of relapse. Increased *MDM2* amplification and messenger RNA (mRNA) expression in dedifferentiated liposarcoma are associated with poorer patient outcomes, further establishing *MDM2* as a crucial biomarker for monitoring liposarcoma.[1,23,24] The *MDM2* gene encodes a ubiquitin ligase that negatively regulates p53.[25,26] The *TP53* gene is vital for cell cycle regulation, apoptosis, DNA repair, and tumor suppression.[27,28] *MDM2*'s role as a genuine human oncogene was confirmed through its amplification across various tumor types[29,30] and in over a third of sarcoma samples.[31] In our study, we assessed *MDM2* (CNV) in blood samples to evaluate

its potential as a biomarker for monitoring disease progression in patients with sarcoma. Sustained activation of the MET proto-oncogene, a receptor tyrosine kinase, transforms osteoblasts into osteosarcoma cells, driving tumor initiation and progression. This central role in osteosarcoma pathogenesis makes MET signaling a crucial biomarker.[32] Chen *et al.*[33] performed genomic profiling on 1,048 sarcoma samples from Chinese patients, discovering 481 gene fusions in 329 cases. They identified *BRAF* fusion events as clinically relevant biomarkers, indicating these events' potential for molecular classification and precision therapy selection in patients with sarcoma. The molecular chaperone heat shock protein 90 (HSP90) regulates multiple critical signaling pathways in cancer by driving the maturation of key signaling components, thereby playing a crucial role in tumorigenesis and drug resistance.[34] Retinoblastoma (*RB1*) alterations, such as gene deletions, are found in bone and STSs and are associated with increased tumor aggressiveness and poorer outcomes.[36] Thus, *RB1* is a critical marker of tumor progression and cell-cycle dysregulation in cancer.

Soft tissue sarcomas remain a group of cancers without any clinically validated circulating biomarker[1], and only a limited number of studies have sought to identify such markers.[1,23,36-38] Extensive, standardized multicenter studies are still needed to facilitate the clinical application of these tools. Our work contributes to these emerging efforts by advancing the investigation of genomic candidates that may ultimately support LB-based monitoring in STS.[1,23,36-38]

The primary objective of our analysis is to identify biomarkers with prognostic potential for patients with sarcoma. We examined human sarcomas to determine whether CNVs in biomarkers (*MDM2, TP53, MET, RB1, BRAF*, and *HSP90*) correlate with clinical prognosis. This work aims to explore a set of biomarkers to quantify their prognostic value during the early phases of STS development and thus identify, as early as possible, potential superior benefits for the patient.

2. Materials and methods

2.1. Materials

Peripheral blood samples were collected into BD Vacutainer® K2EDTA Blood Collection Tubes (Becton, Dickinson and Company, United States of America [USA]). cfDNA was isolated using the QIAamp® Circulating Nucleic Acid Kit (55114, Qiagen GmbH, Germany). DNA concentration and purity were assessed by measuring absorbance at 230, 260, and 280 nm using a Spark® Multimode microplate reader (Tecan Group Ltd., Switzerland).

Copy number variation analysis was performed using the QX200™ Automated Droplet Generator and QX200™ Droplet Reader (Bio-Rad Laboratories Inc., USA). Droplets were generated using ddPCR™ Droplet Generation Oil for Probes (186-3005, Bio-Rad Laboratories Inc.). PCR was performed using ddPCR™ Supermix for Probes (No dUTP) (1863023, Bio-Rad Laboratories Inc.).

The following ddPCR™ Copy Number Assays (Bio-Rad Laboratories Inc.) were used: *MET* (dHsaCP1000038), *RB1* (dHsaCP1000052), *BRAF* (dHsaCP2506666), *HSP90AB1* (dHsaCNS438853620), *TP53* (dHsaCP1000586), and *MDM2* (dHsaCP2500317). Gene copy number was normalized using the AP3B1 Copy Number Reference Assays (Bio-Rad Laboratories Inc.): dHsaCP1000001 (*MET*, *RB1*, and *MDM2*), dHsaCP2500315 (*BRAF*), and dHsaCP2500348 (*HSP90AB1* and *TP53*).

We performed PCR amplification using a C1000 Touch™ Thermal Cycler (Bio-Rad Laboratories Inc.). Data acquisition and analysis were performed using QuantaSoft™ software version 1.7 (Bio-Rad Laboratories Inc.). Nuclease-free water was purchased from Thermo Fisher Scientific (USA) and used for all PCR experiments.

2.2. Methods

2.2.1. Patient population

A prospective study was conducted, including 19 patients with histologically confirmed primary high-risk STS who underwent uniform treatment with neoadjuvant radiotherapy (RTh) and chemotherapy (ChTh), followed by surgical resection between 2023 and 2025. High-risk STS refers to STSs with a high likelihood of recurrence and metastasis, typically associated with high histological grade, tumor diameter >5 cm, deep location relative to the fascia, and an overall 10-year survival probability <60% according to SARCULATOR (https://www.sarculator.com/). Risk stratification was based primarily on histological subtype, tumor grade, size, and anatomical location. High-risk patients, typically those with intermediate- or high-grade tumors, most often relapse within the first 2–3 years after treatment, whereas low-risk patients may relapse later. High-grade STSs are therefore a clinically aggressive subgroup that requires closer surveillance and often more intensive therapeutic management.[38,39]

Neoadjuvant treatment and surgery were recommended after a multidisciplinary tumor board that evaluated factors connected with the patient, such as age, comorbidities, and Eastern Cooperative Oncology Group (ECOG) scale, and factors connected with the tumor, such as the risk of positive margins, tumor location, grade, size, and histopathologic subtype. Exclusion criteria were under 18 years of age, recurrent sarcoma, metastatic disease at

diagnosis, retroperitoneal STS, bone sarcomas (e.g., Ewing's sarcoma, chondrosarcoma, osteosarcoma), and benign or intermediate histological subtypes, such as aggressive fibromatosis, desmoid tumor, and dermatofibrosarcoma protuberans. For all 19 recruited patients, complete resected specimen slides were available for re-evaluation in the final analysis.

Tumors were resected with a wide margin of surrounding healthy tissue, aiming to achieve complete resection with a negative surgical margin. No specific recommendation for the width of that margin was used, in accordance with current guidelines. Staging was conducted according to the 8th edition of the AJCC system. Histologic type and grade were reported using the World Health Organization (WHO) classification and the French National Federation of Cancer Centers (FNFCC) system, based on biopsy results obtained prior to treatment. Molecular features were not used alongside histopathological findings to aid the diagnosis of sarcoma histologic subtype. Grades 2 and 3 tumors in the FNFCC system were classified as "high grade," whereas grade 1 tumors were classified as "low grade."

2.2.2. Radiotherapy and chemotherapy treatment protocol

Chemotherapy was given in three cycles of doxorubicin and ifosfamide, each every three weeks; RTh was given between the first and second cycles of ChTh (Figure 1). The treatment, according to the protocol, included preoperative hypofractionated RTh.[39] Administration of preoperative RTh was conducted in the following scheme: five fractions of 6 Gy each prescribed for the average planning target volume (PTV) or appropriate isodose up to a total dose of 30 Gy over five consecutive days, with possible dose escalation to the tumor in the form of a boost to 7 Gy, up to a total dose of 35 Gy. RTh was given with or without simultaneous hyperthermia treatment in a regimen of twice a week with a minimum one-day break between. Hyperthermia is a local treatment with low toxicity that, when combined with RTh and ChTh, has shown improved local control rates and disease-free survival in preliminary evaluations in patients with STS (SINDIR study).[40,41] The details of RTh, such as dose and technique, as well as potential combination with hyperthermia, were provided by an RTh specialist. Hyperthermia treatment duration, energy, and temperature were determined in accordance with the hyperthermia treatment protocol. All patients received treatment according to the ChT–RTh–ChTh–ChTh regimen. However, not all patients received hyperthermia. The administration of hyperthermia depended on clinical feasibility (e.g., anatomical conditions) as well as on technical capabilities and workflow organization, including availability of the hyperthermia device throughout RTh.

Preoperative systemic ChTh was used on an individual basis in selected cases of STS, after assessing tumor features such as degree of malignancy, chemosensitivity, and local

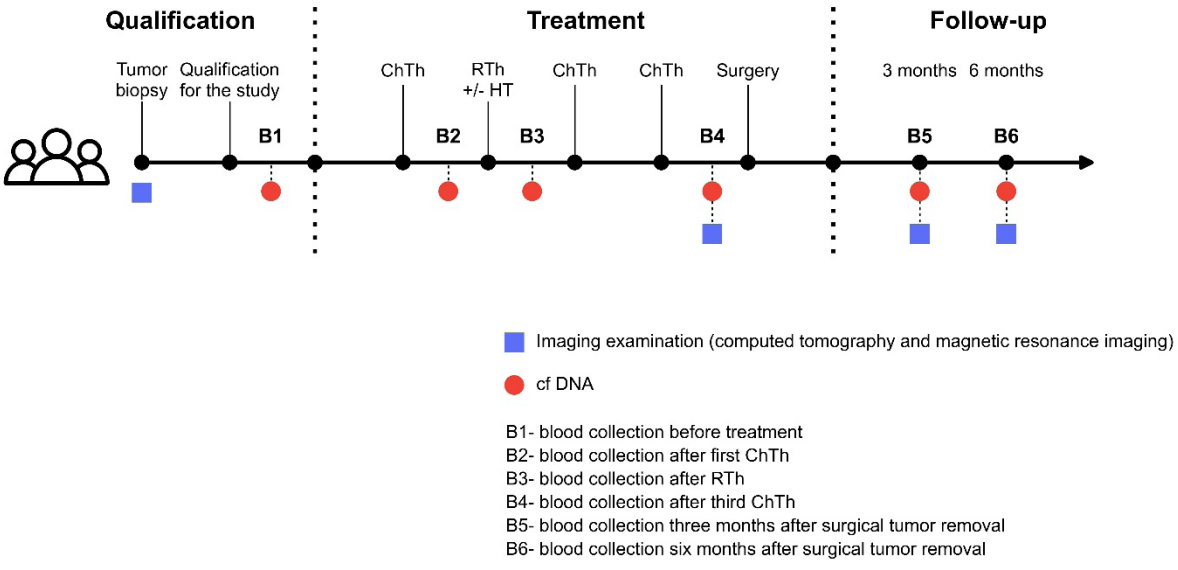


Figure 1. Treatment and follow-up timeline
Abbreviations: cf: Cell-free; ChTh: Chemotherapy; HT: Hyperthermia; RTh: Radiotherapy.

advancement, as well as the patient's general condition. Based on these factors, the risk of tumor metastasis and recurrence was assessed. Typically, ChTh was based on anthracyclines (e.g., doxorubicin) as monotherapy or in combination with other drugs.

The treatment regimen included ChTh–RTh–ChTh–ChTh, and two to three weeks after completing preoperative radiochemotherapy, the response to treatment was assessed by the referring surgeon-oncologist to determine eligibility for surgery. Using such a treatment regimen allows high rates of local disease control with few late toxicities.

In detail, all patients received three courses of preoperative ChTh prescribed as part of their preoperative treatment. Ten of the 19 patients received concurrent hyperthermia during RTh. Surgery was performed between the 9th and 11th week after the start of the first course of ChTh. All patients received preoperative ChTh and RTh. All patients underwent surgery in accordance with the treatment plan.

2.2.3. Pathologic evaluation and response

The surgical specimens after radiochemotherapy were handled in accordance with the College of American Pathologists guidelines.[42] Each slide's percentages of viable tumor cells, necrosis, and fibrosis/hyalinization were evaluated, and the total percentage for each component was computed across the entire specimen to ensure the three components added up to 100%. Stainable, aberrant tumor cells with hyperchromatic nuclei, smeared and clumped chromatin, cellular and nuclear pleomorphism, large nucleoli, abnormal and odd mitoses, loss of tissue polarity, and increased cellular size were considered viable. Necrosis was measured as confluent regions of degenerate cells, karyorrhectic nuclear debris, polymorphonuclear neutrophil infiltrate, and necrotic tumor cells (preserved cellular outline "ghost" cells with loss of nuclear stain). Hypocellular regions with thick, uniform, amorphous deposition of eosinophilic material, with or without a dense collagenous matrix including fibroblasts, were used to quantify fibrosis/hyalinization.

The European Organization for Research and Treatment of Cancer-Soft Tissue and Bone Sarcoma Group (EORTC-STBSG) score, which classifies the percentage of live cells in the resection specimen as follows, was used to categorize the pathologic response to neoadjuvant treatment: Grade A: no viable tumor cells; Grade B: single viable tumor cells or small clusters (less than 1% of the specimen); Grade C: ≥1% to <10% viable tumor cells; Grade D: ≥10% to <50% stainable tumor cells; and Grade E: ≥50% viable tumor cells. The proportion of necrosis and the degree of fibrosis/hyalinization in the removed material were used to evaluate the pathologic response. Less than or equal to 5% of viable tumor cells was considered pathologic complete response. The pathologic response was also evaluated using a combination of the percentage of viable tumor cells and treatment-related changes (such as fibrosis or hyalinization). If at least 10% of the tumor mass showed treatment-related changes, the response was classified as "very good" or "good," with "very good" denoting less than 10% viable tumor cells and "good" denoting 10% to 50% viable tumor cells. Patients were categorized as non-responders if they did not fit these requirements.

2.2.4. Acquisition and processing of blood samples, plasma isolation, and cfDNA extraction

Peripheral blood samples were collected from 19 patients diagnosed with STS at the Maria Sklodowska-Curie National Research Institute of Oncology (NIO, Warsaw, Poland). The study procedures were conducted in compliance with the approval granted by the Ethics Committee at NIO (protocol code No. 53/2024) and in accordance with the Declaration of Helsinki. Written informed consent was obtained from all participants, and the procedures were carried out in accordance with institutional guidelines. After giving consent, approximately 10 mL of whole blood was collected into blood collection tubes. Blood samples were collected from patients at six time points: at qualification (before starting treatment; B1 in Figure 1), followed by collection at the next three points during treatment (after first ChTh, mostly on the day of starting RTh [B2], after RTh, mostly the day before starting second ChTh [B3], after third ChTh, mostly 1–2 days before surgery [B4]), and after that, three (B5) and six months (B6) following surgical tumor removal. The exact treatment timeline and corresponding blood collection schedule are presented in Figure 1. Blood samples were shipped at room temperature and processed within 24 h using a double-centrifugation protocol (1,900 × *g* for 10 min at 4 °C) to maximize plasma recovery and remove any remaining blood cells. cfDNA was isolated from the plasma using the QIAamp Circulating Nucleic Acid Kit. The quantity and purity of the isolated cfDNA were assessed spectrophotometrically by measuring absorbance at 230 nm, 260 nm, and 280 nm using a Spark Multimode microplate reader.

2.2.5. Biomarker copy number qualification

Copy number variations of six target genes: *MET*, *RB1*, *BRAF*, *HSP90AB1*, *TP53*, and *MDM2* were assessed using droplet digital PCR (ddPCR). The PCR mixture was prepared by combining 10 µL of ddPCR™ Supermix for Probes (No dUTP), 1 µL of the specific ddPCR™ Copy Number Assay, 1 µL of the reference sequence assay, 5 µL of nuclease-free water, and 5 µL of isolated cfDNA. AP3B1 Copy Number Reference Assays, recommended

by the manufacturer for the Bio-Rad ddPCR copy number workflow, were included in the relevant CNV analyses as a stable diploid reference locus for normalizing target copy number. Stable reference assay performance was observed throughout the study, with no evidence of technical instability.

Droplets were generated using a Bio-Rad® QX200 Automated Droplet Generator with ddPCR™ Droplet Generation Oil for Probes. PCR amplification was carried out using the following thermal cycling profile: a 3-min hold at 25 °C, followed by polymerase activation at 95 °C for 10 min. Subsequently, 40 amplification cycles were performed, each consisting of denaturation at 94 °C for 30 s and a combined annealing/extension step at 60 °C for 1 min. After cycling, the reaction was subjected to polymerase deactivation at 98 °C for 10 min. The protocol concluded with a 30-min hold at 12 °C, followed by indefinite storage at 8 °C until further processing. All temperature transitions were performed at a ramp rate of 2 °C/s. Following amplification, the concentration of each target gene in the reaction mixture was determined using the QX200 Droplet Reader.

Each ddPCR Copy Number Assay included a target-specific 6-carboxyfluorescein (FAM)-labeled probe and a hexachloro-6-carboxyfluorescein (HEX)-labeled reference probe in accordance with the manufacturer's recommendations. Therefore, copy number estimates were normalized to a stable reference locus, with CNV values calculated as the ratio of target-gene copies to reference-gene copies, following the manufacturer's recommendations. QuantaSoft software automatically reported the absolute target concentration (copies/µL reaction) based on Poisson analysis of accepted droplets. These values were subsequently converted to copies/mL plasma using **Equation 1**.

$$c = \frac{c_{ddPCR} \cdot V_{elu} \cdot X \cdot V_m}{V_{ana} \cdot V_p} \quad (1)$$

where c is the concentration of gene in plasma (copies/mL); c_{ddPCR} is the concentration of the gene in PCR reaction mix; V_{elu} is the total volume of cfDNA isolated from plasma; X is the cfDNA dilution factor; V_{ana} is the volume of cfDNA used in PCR reaction mix; V_m is the total volume of PCR reaction mix; and V_p is the initial volume of plasma used for isolation.

Droplet generation was considered acceptable when each reaction produced at least 10,000 accepted droplets, while reactions with <10,000 accepted droplets were excluded and repeated. Fluorescence amplitude thresholds distinguishing positive from negative droplets were determined individually for each assay based on the separation of positive and negative droplet clusters and were held constant across all samples analyzed in the same experimental run. Each ddPCR run included the following quality controls: no-template controls (NTCs) to monitor contamination, and reference gene assays for normalization and assessment of DNA quality. Runs were considered valid only when NTCs showed no positive droplets.

2.3. Statistical analysis

Statistical analyses were performed using R (v.4.4.3). Continuous variables are presented as median and interquartile range (IQR), whereas categorical variables are presented as counts and percentages. Given the limited sample size and the lack of assumptions about the normality of the variables analyzed, non-parametric statistical methods were applied throughout the study. Differences between two independent groups were assessed using the two-sided Wilcoxon rank-sum test. Correlations between variables were evaluated using Spearman's rank correlation coefficient. For analyses involving multiple biomarkers measured simultaneously, p-values were adjusted for multiple comparisons using the Benjamini–Hochberg (BH) procedure to control the false discovery rate. Both nominal (unadjusted) and BH-adjusted p-values were considered during interpretation. Unless otherwise stated, statistical significance was defined as an adjusted p-value < 0.05. Progression-free survival (PFS) was defined as the time from treatment qualification to documented disease progression or last follow-up. Survival curves were estimated using the Kaplan–Meier method and compared using the log-rank test. To identify candidate prognostic thresholds for biomarker CNV at time points B2 and B3, a threshold optimization procedure was applied. For each biomarker, 400 equally spaced candidate thresholds within the observed range were evaluated. Thresholds generating groups with fewer than three patients were excluded. For each candidate threshold, patients were dichotomized into low- and high-CNV groups and compared using the log-rank test. The threshold corresponding to the minimum log-rank p-value was selected as the optimal threshold. The resulting p-values were further BH-adjusted. Because threshold selection and performance evaluation were performed using the same dataset, these analyses should be regarded as exploratory and hypothesis-generating.

3. Results

3.1. Patient characterization and tumor characteristics

The demographic and clinicopathological details of the studied patient cohort are presented in Table 1. There were 10 female patients and 9 male patients, with a median age

of 47 years (IQR: 40–60 years). The STS was located in the lower limb in 14 patients (74%), in the pelvis in 2 patients (10%), and in other localizations: upper limb, breast, and abdominal wall. Nine patients (47%) had tumor volume greater than 1,000 cm^3, while nine patients (47%) had tumor volume smaller than or equal to 500 cm^3. Eight patients (42%) had undifferentiated pleomorphic sarcoma, 4 (21%) had synovial sarcoma, 2 (10%) had myxoid liposarcoma, and 5 (26%) had other STS subtypes. Malignant peripheral nerve sheath tumor, leiomyosarcoma, pleomorphic rhabdomyosarcoma, malignant tenosynovial giant cell tumor, and myogenic sarcoma were other less common histological categories. None of the patients had low-grade tumors, and three patients (16%) had G2 tumors; the remaining patients (16, 84%) had G3 tumors. Seventeen patients (89%) had R0 resection, while two patients (10%) had R1. There were no R2 resections.

3.2. Post-treatment pathological characteristics

The pathologic characteristics of the resected tumors stratified by histological subtype are presented in Table 2. The median percentages of viable cells were 8.5% (IQR: 1.25%–35.00%), and necrosis/fibrosis was 91.5% (IQR: 65.00%–98.75%). Table 2 also shows the pathologic treatment response, stratified by histological subtype and categorized by the EORTC-STBSG score. Grade D accounted for 32% of instances, Grade C for 26%, and Grade B for 21%. Meanwhile, 5% of the cases had total tumor cell elimination (Grade A). Eight patients (42%) showed a pathologic complete response. Two patients (10%) had a "very good" pathologic response, six patients (32%) had a "good" response, and three patients were categorized as non-responders.

3.3. Correlation analysis of copy number variations of key cancer-related genes (*TP53, RB1, MDM2, BRAF, MET,* and *HSP90)* and clinical parameters across time points (B1–B6)

A set of correlations emerged between clinical outcomes and molecular markers (Figure 2). Continuous variables included biomarker measurements (*MDM2*, *TP53*, *RB1*, *MET*, *BRAF*, *HSP90*), tumor volume, and percentage of necrosis or fibrosis. Treatment response was represented by one of the five grades of the EORTC-STBSG score. The progression status was treated as a dichotomous variable (progression vs. no progression). Tumor size showed a slight correlation with disease progression and with CNVs in the biomarker *BRAF* at time point B4. Additionally, disease progression showed substantial correlations with CNVs of *MDM2* and *MET* at time point B2, and with CNVs of *TP53, RB1, MDM2,* and *HSP90* at time point B3. In contrast, necrosis was negatively correlated with *TP53* CNVs at time point B6. However, those correlations did not reach the significance threshold after adjustment for multiple testing using the BH test.

Table 1. Demographic and clinicopathological characteristics of the studied patient cohort (*N* = 19)

Characteristic	*n* (%)
Age at diagnosis (years; median [IQR])	40–60
Sex	
Female	10 (53)
Male	9 (47)
Histologic subtype	
UPS	8 (42)
SS	4 (21)
MLS	2 (10)
Other	5 (26)
Tumor grade	
G1	0 (0)
G2	3 (16)
G3	16 (84)
Tumor location	
Lower limb	14 (74)
Pelvis	2 (10)
Upper limb	1 (5)
Breast	1 (5)
Abdominal wall	1 (5)
Tumor volume (cm^3)	
<500	9 (47)
≥500 and <1,000	1 (5)
>1,000	9 (47)
Resection margin	
R0	17 (89)
R1	2 (10)
R2	0 (0)
Hyperthermia	
Yes	11 (58)
No	8 (42)

Note: Other histologic subtypes included malignant peripheral nerve sheath tumor, leiomyosarcoma, pleomorphic rhabdomyosarcoma, malignant tenosynovial giant cell tumor, and myogenic sarcoma. Abbreviations: IQR: Interquartile range; MLS: Myxoid liposarcoma; SS: Synovial sarcoma; UPS: Undifferentiated pleomorphic sarcoma.

Table 2. Pathologic characteristics after neoadjuvant treatment and response assessment using the EORTC-STBSG score stratified by STS histological subtype (*N* = 19)

Characteristics	*n* (%)
Treatment results	
Viable (%, median [IQR])	8.5 (1.25–35.00)
Necrosis/Fibrosis (%, median [IQR])	91.5 (65.00–98.75)
EORTC-STBSG score	
A	1 (5)
B	4 (21)
C	5 (26)
D	6 (32)
E	3 (16)

Note: EORTC-STBSG scores: A: No viable cells; B: Single viable tumor cells or small clusters (<1%); C: ≥1% to <10% viable tumor cells; D: ≥10% to <50% viable tumor cells; E: ≥50% viable tumor cells.
Abbreviations: EORTC-STBSG: European Organization for Research and Treatment of Cancer-Soft Tissue and Bone Sarcoma Group; IQR: Interquartile range;

Serial cfDNA measurements demonstrated moderately positive correlations between consecutive sampling time points, suggesting a temporal stability of cfDNA levels during treatment. Correlations were strongest between adjacent time points (particularly B2–B4), whereas associations appeared to weaken between more distant measurements. Notably, later cfDNA measurements showed a tendency for positive correlation with disease progression and negative correlation with treatment response. These observations may support the use of longitudinal cfDNA monitoring as a potential marker of treatment outcome, warranting further investigation in larger, prospective studies.

Significant correlations between biomarkers were observed at both different time points and within the same time points. Generally, biomarkers (CNVs) at each time point correlated with one another, with only a few exceptions that did not reach statistical significance (i.e., *BRAF* with *MET* and *HSP90* at B1, and *HSP90* with *TP53* at B4). Biomarkers measured after ChTh (B2) correlated with those measured after RTh (B3) (Figure 2).

Moreover, CNVs after the third ChTh (B4), directly before surgery, correlated with CNVs at three months after surgery (B5), but only some of the correlation coefficients reached significance (Figure 2). We observed a weak negative correlation between measurements collected at B2/B3 and those at B5. These negative correlations suggest that there are variations in measurements during and after therapy. A weak negative correlation was observed between biomarkers at B5 and B6 (Figure 2). Measurements at B4, at the end of therapy, tended to be negatively correlated with those at six months after surgery (B6). Some of them were significant (Figure 2). A negative correlation reflected differences in biomarker levels between the two time points (B4 vs. B6), including an increase for Patient 5 (who did not experience progression) and for Patient 9 (who did experience progression), as shown in Figure 3 and Figure S1. Missing molecular measurements by assessment time points, where percentages were calculated relative to the total cohort, and missing measurements by patient, where percentages were calculated across 46 variables per patient, are presented in Tables S1 and S2.

3.4. Copy number variations of oncogenic drivers in relation to disease progression and EORTC-STBSG treatment response in B1

For the study, EORTC-STBSG response categories were divided into non-responders (E) and responders (A, B, C, and D) to compare genomic CNV profiles before therapy (at the qualification, B1) in patients with and without durable therapeutic benefit (Figure 4). This approach was selected to distinguish patients demonstrating histopathological evidence of treatment effect from those with minimal or no pathological response. Given the limited cohort size, further subdivision of patients into alternative response categories, such as A–C versus D–E or pathological complete response versus non-pathological complete response, would have substantially reduced statistical power and resulted in very small subgroup sizes. Therefore, the observed associations between circulating CNV profiles and treatment response should be regarded as exploratory and require validation in larger, independent cohorts using alternative clinically relevant response classifications.

Notably, an increase in *MDM2* CNV was observed in non-responders in the unadjusted Wilcoxon rank-sum test, suggesting its link to poor therapeutic outcomes. However, after the BH correction for multiple testing, this association was no longer statistically significant at the 0.05 threshold. Therefore, the observed baseline difference in *MDM2* CNV should be interpreted as a preliminary signal rather than definitive evidence of association with treatment response.

3.5. Association of *TP53, RB1, MDM2, BRAF, MET,* and *HSP90* copy number variations at different time points (B1–B6) with disease progression

The genes *TP53, RB1, MDM2, BRAF, MET*, and *HSP90* (CNV) were compared pairwise across six consecutive time points (B1–B6; Figure 5). Generally, a slight increase

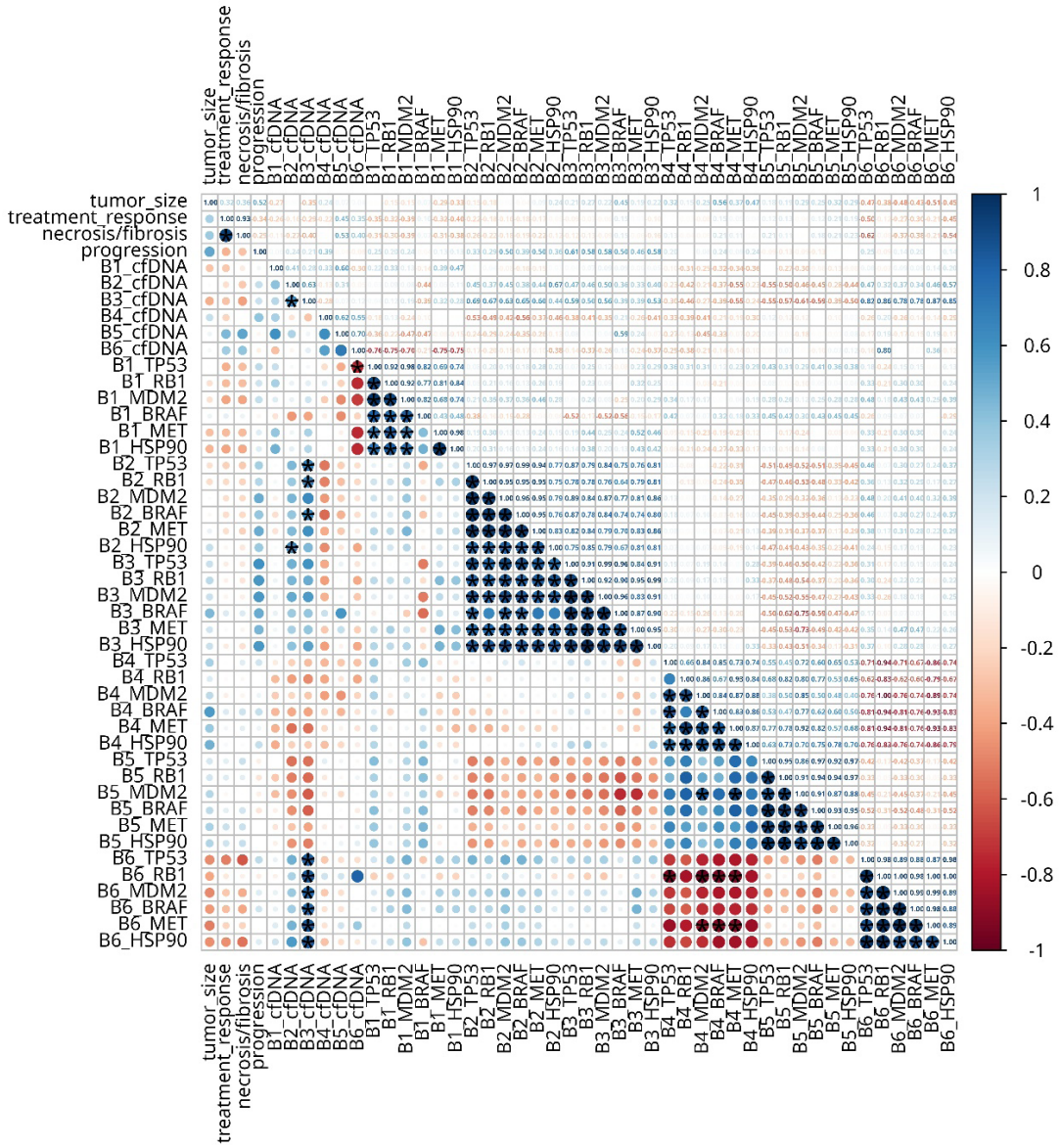


Figure 2. Time-dependent correlation matrix of genomic and clinical parameters (B1–B6). Spearman correlation matrix showing relationships between copy number variations (CNVs) of *TP53*, *RB1*, *MDM2*, *BRAF*, *MET*, and *HSP90* as well as cfDNA at different time points (B1–B6), and selected clinical parameters (tumor size, necrosis/fibrosis, treatment response, and disease progression) across all patients. Colors indicate the direction and strength of correlations (blue: positive, red: negative), with color intensity reflecting the magnitude of the correlation coefficient. Lower triangle: the areas of circles show the absolute value of corresponding correlation coefficients. Upper triangle: values of the correlation coefficients. Note: *BH-adjusted $p < 0.05$.

in CNVs at the cohort level was noted only after B2 for *TP53, MDM2,* and *HSP90* compared with B1. Notably, we identified changes in biomarker CNV levels at specific time points during therapy between patients with different disease progression statuses, even though all progressions were noted after the end of therapy (after B4). Patients who later progressed tended to show higher *MDM2* and *MET* CNV after ChTh (B2) than those without progression. Similarly, after RTh (B3), they have increased *TP53, RB1, MDM2,* and *HSP90* CNVs. However, after BH correction for multiple testing, none of these comparisons remained statistically significant at the 0.05 threshold. Therefore, these findings should be interpreted with caution and require confirmation in larger independent cohorts.

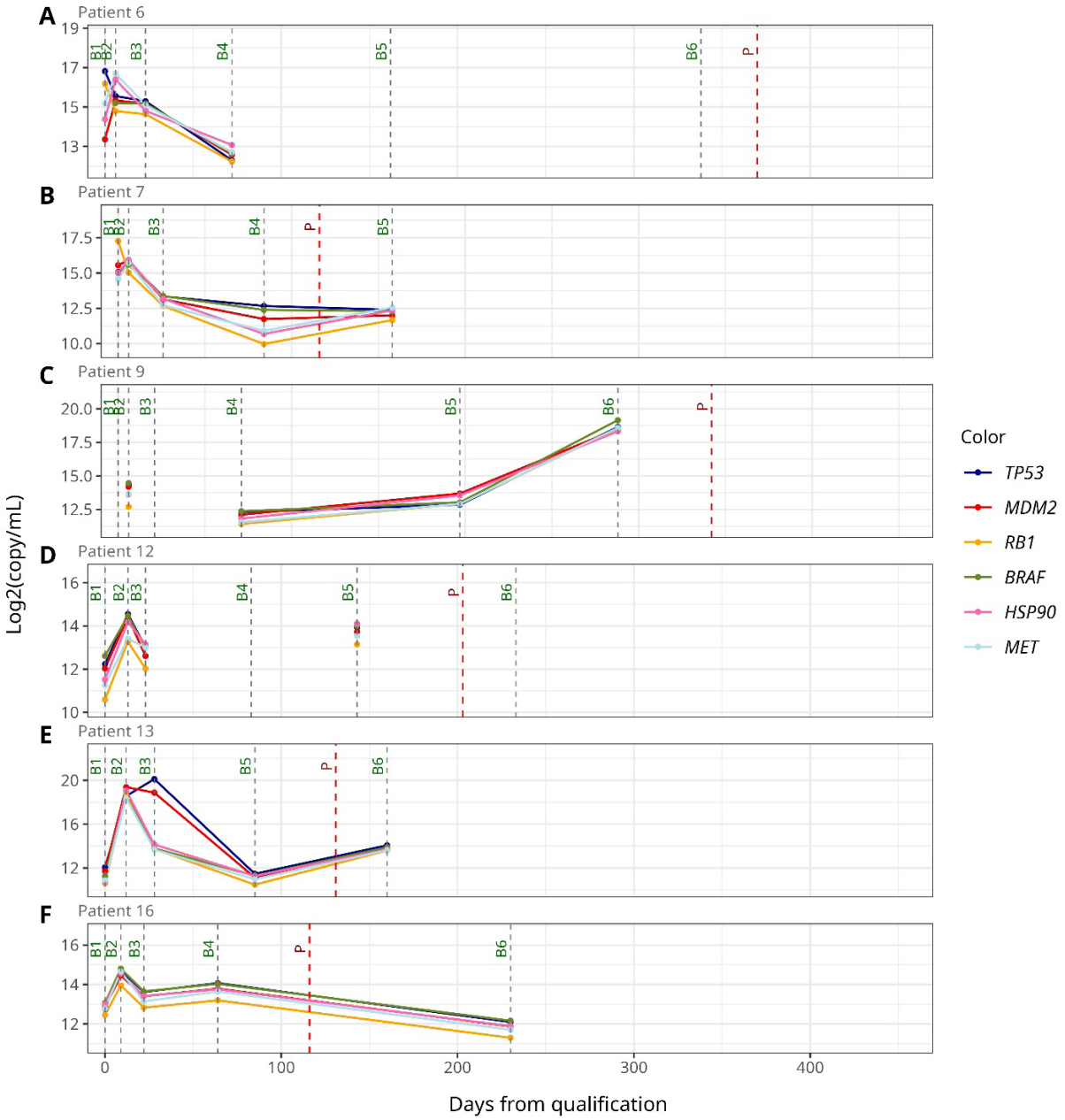


Figure 3. Longitudinal analysis of $\log_2$-transformed copy number variations for selected genes (*BRAF, HSP90, MDM2, MET, RB1,* and *TP53*) measured across sequential liquid biopsies in individual patients with progression. Each panel represents one patient, with colored lines indicating different genes. The x-axis shows days from qualification, and the y-axis shows $\log_2$ (copy/mL). Vertical black dashed lines indicate blood sample collection at examination time points (B1–B6), and the red dashed line indicates the time point of disease progression (P). (A) Patient 6. (B) Patient 7. (C) Patient 9. (D) Patient 12. (E) Patient 13. (F) Patient 16.

3.6. Time-point-specific density distributions of plasma biomarkers in relation to disease progression: Identification of optimal prognostic cut-off values for *TP53, RB1* and *MDM2*

We focused on measurements during therapy (B2 and B3), noting differences in disease progression between patients. The analysis of density distributions of plasma CNVs for *TP53, RB1, MDM2, BRAF, MET,* and *HSP90* after ChTh and after RTh revealed consistent rightward shifts in patients who progressed compared to those who did not

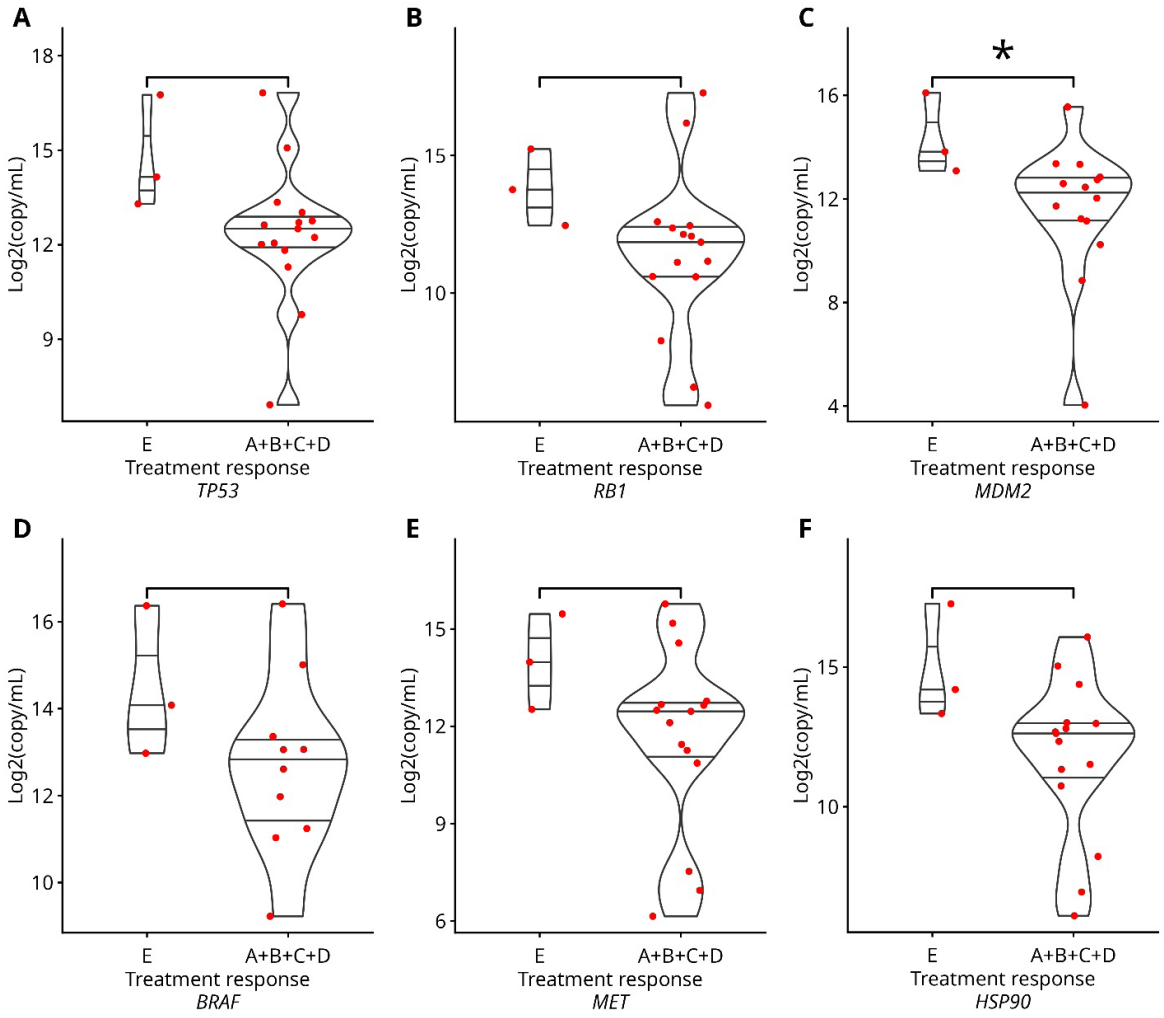


Figure 4. Association of gene copy number variations (CNVs) with treatment response at time point B1 according to EORTC-STBSG criteria. Violin plots showing CNVs of (A) *TP53,* (B) *RB1,* (C) *MDM2,* (D) *BRAF,* (E) *MET,* and (F) *HSP90* in relation to treatment response according to EORTC-STBSG criteria (categories A–E). For statistical analysis, the categories were dichotomized into non-responders (category E) and responders (categories A–D). Red dots represent individual patient samples, while the width of the violins reflects the data distribution, with the lower line indicating the first quartile, the middle line indicating the median, and the upper line indicating the third quartile. * indicates unadjusted p-value < 0.05 (BH-adjusted p-values were not significant).

(Figure 6). The strongest separation between progressors and non-progressors was noted for *TP53, MDM2, MET,* and *HSP90* in B2 and for *RB1* and *HSP90* in B3.

The optimal threshold for biomarkers measured in B2 and B3 to discriminate between patients with different PFS was estimated. The log-rank test was used to assess differences in PFS curves between two groups: patients with biomarker measurements equal to or above the threshold and those with measurements below the threshold. Different thresholds were tested within the allowed range to separate all patients into two groups with at least three patients in each group (allowing for too-small groups is very sensitive to outliers that may give artificially low p-values; Figure 7). Threshold analysis of biomarkers measured at B2 and B3 identified distinct minima in the log-rank p-value profiles for most analyzed genes. At B2, clear minima were observed for *TP53, MDM2, BRAF, MET*, and *HSP90*, whereas *RB1* showed a less pronounced minimum. At B3, all analyzed biomarkers displayed well-defined minima, enabling the identification of candidate CNV cut-off values (Figure 8). In the unadjusted analysis, several of these thresholds were associated with differences in PFS. However, after BH correction for multiple testing, none of the associations remained statistically significant at the 0.05 threshold. Kaplan–Meier analysis nevertheless

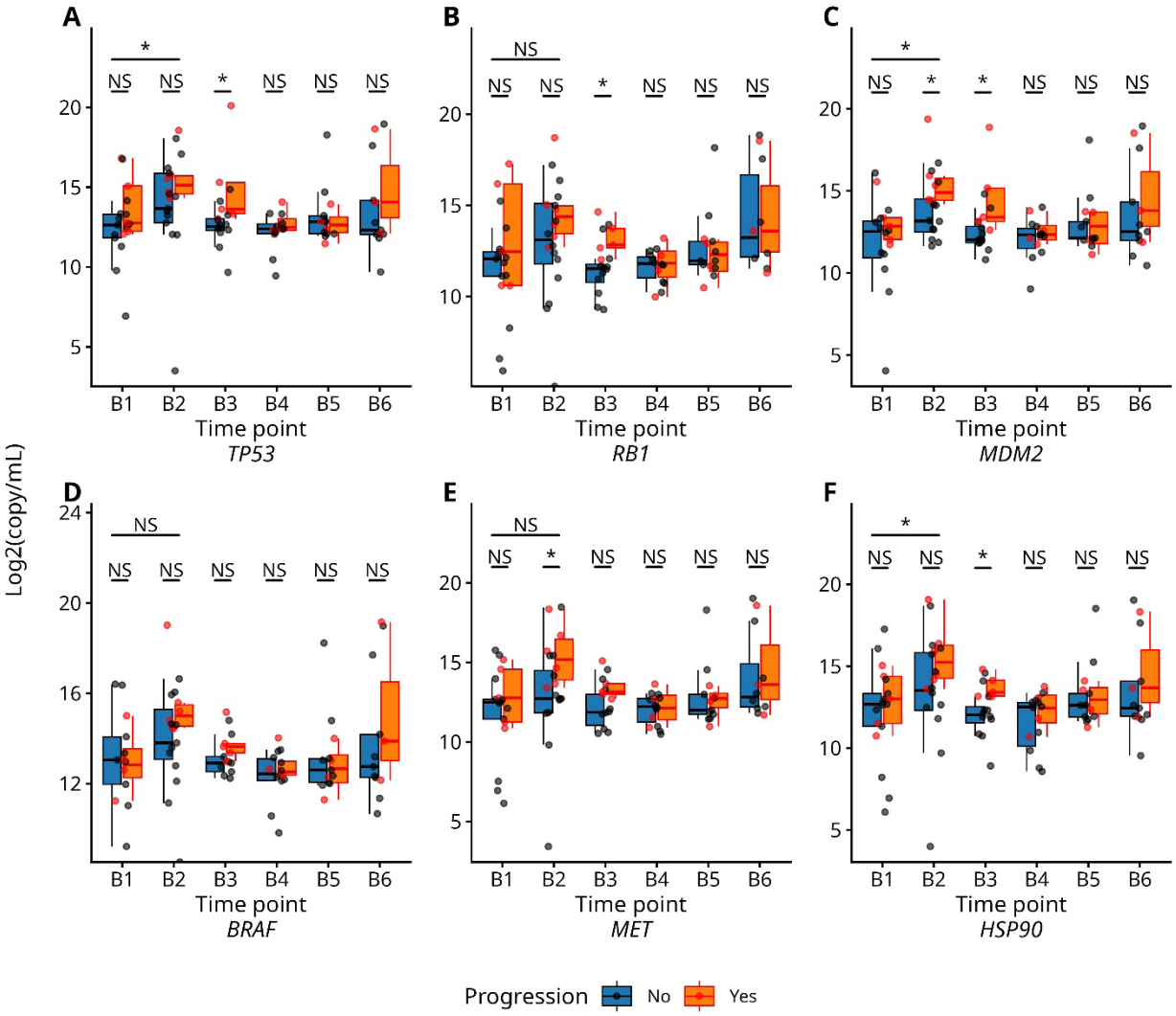


Figure 5. Copy number variations (CNVs) of (A) *TP53,* (B) *RB1,* (C) *MDM2,* (D) *BRAF,* (E) *MET,* and (F) *HSP90* across consecutive blood collection time points (B1–B6). For each biomarker, comparisons were performed between all pairs of time points. For clarity, lines with significance levels are shown only for comparisons between B1 and B2, where changes are observed. Differences between patients with (blue boxplot, black dot) and without (yellow boxplot, red dot) disease progression are marked for each time point. Wilcoxon two-sided rank-sum test was used; *unadjusted $p < 0.05$; NS (Not significant) denotes $p > 0.5$. After Benjamini–Hochberg adjustment for multiple testing across the biomarkers presented in this figure, no comparison remained statistically significant at the 0.05 threshold.

suggested a tendency toward earlier disease progression in patients with higher CNV levels. Correspondingly, high-CNV groups tended to show a steeper decline in PFS, whereas low-CNV groups generally maintained more stable PFS. Therefore, the identified cut-off values should be considered preliminary and interpreted with caution. Given that threshold selection and performance assessment were conducted in the same cohort, these findings require validation in independent datasets before any clinical application can be considered.

4. Discussion

Advances in genomics, together with improved LB technologies, are accelerating efforts to identify reliable markers that could support diagnosis, prognostication, and assessment of treatment response in STS.[1] We examined tumor size, treatment response, necrosis, progression, and six CNV biomarkers (*TP53, MDM2, RB1, BRAF, MET,* and *HSP90*) to determine their roles and potential prognostic significance.

The correlations between clinical outcomes and specific

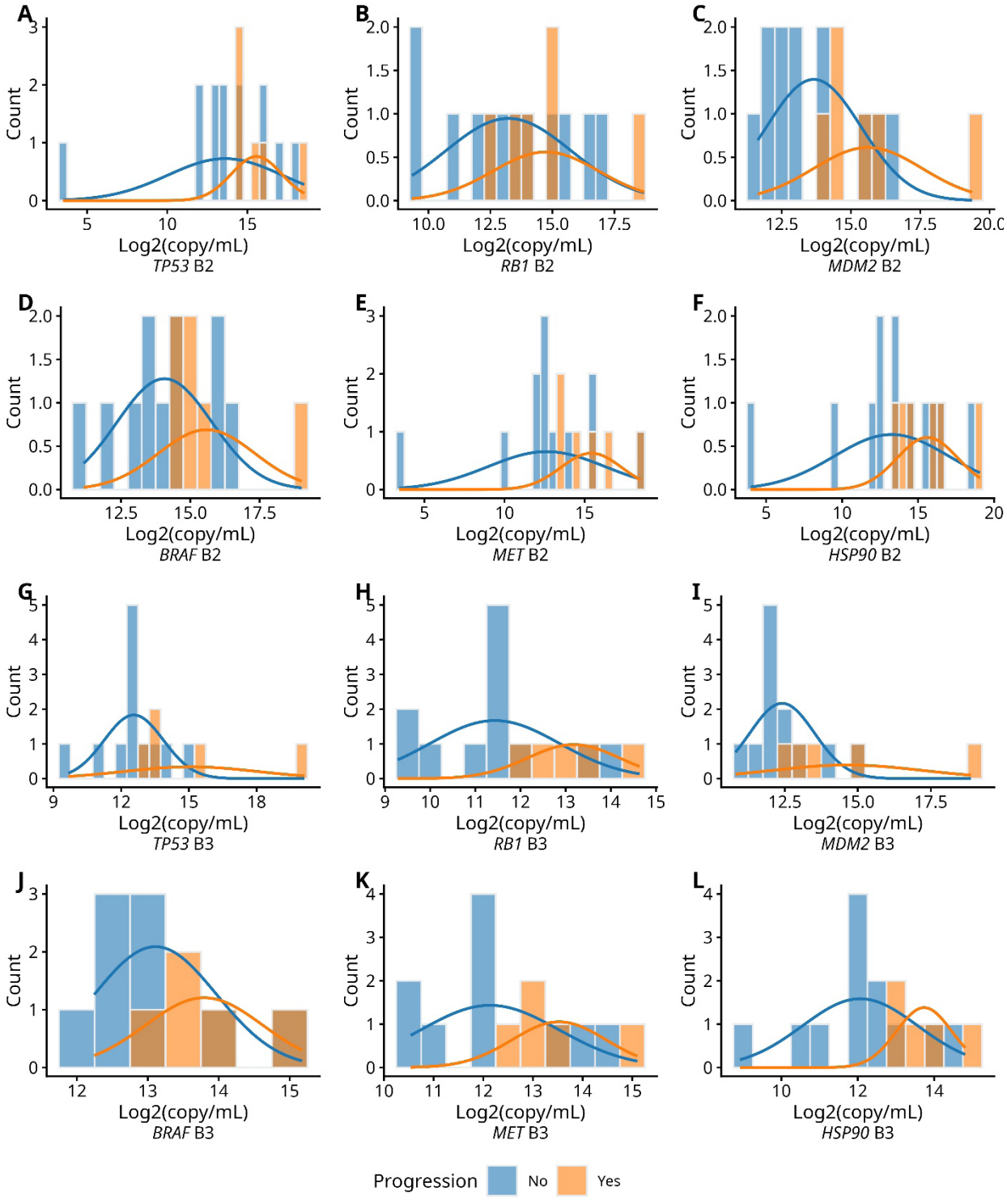


Figure 6. Histograms of plasma *TP53, RB1, MDM2, BRAF, MET,* and *HSP90* copy number variations in patients without disease progression (blue) and with disease progression (orange) at the blood collection time points B2 and B3. The x-axis is shown on a logarithmic scale. Continuous lines represent Gaussian distributions fitted to the histograms. (A) *TP53*, (B) *BRAF*, (C) *RB1*, (D) *MET*, (E) *MDM2*, and (F) *HSP90* at B2, and (G) *TP53*, (H) *BRAF*, (I) *RB1*, (J) *MET*, (K) *MDM2*, and (L) *HSP90* at B3.

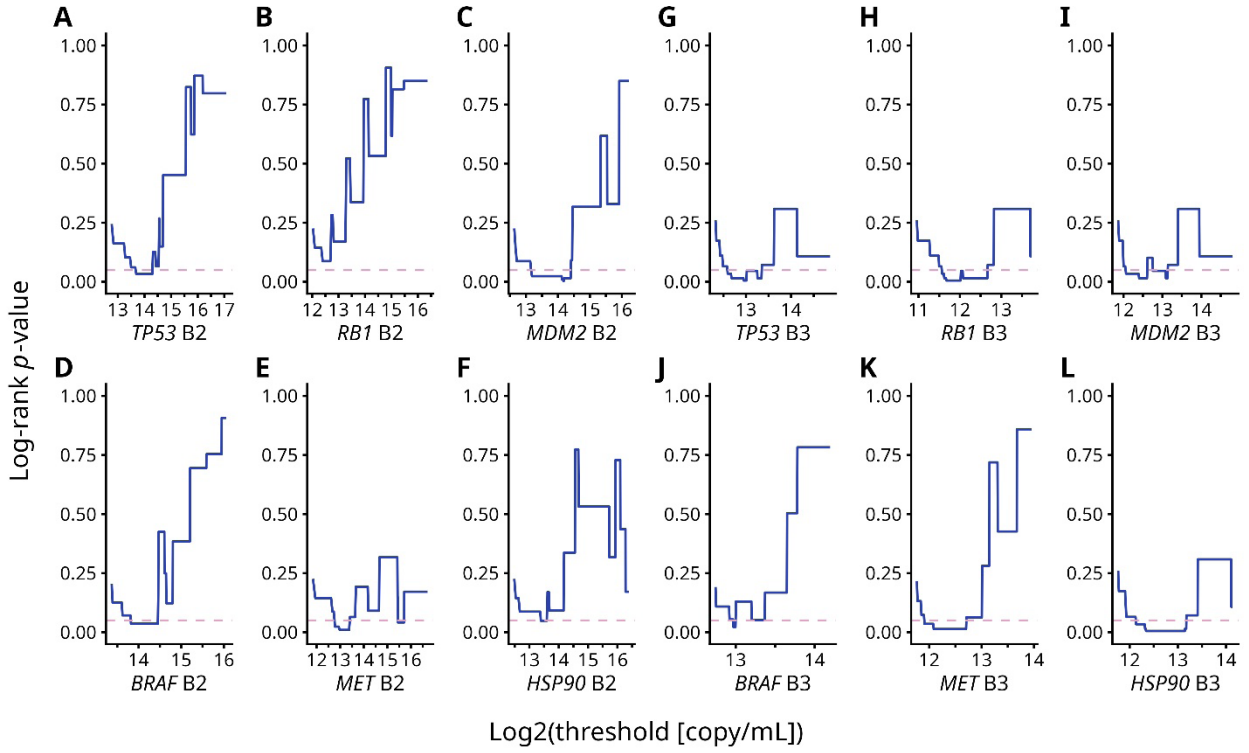


Figure 7. Determination of optimal copy number variation thresholds for *TP53, RB1, MDM2, BRAF, MET,* and *HSP90* at B2 and B3. Threshold-dependent progression-free survival (PFS) curve differences, measured by *p*-values from log-rank test profiles, are shown for two groups of patients obtained by applying different threshold values of *TP53, RB1, MDM2, BRAF, MET,* and *HSP90* at B2 and B3 (copies/ml on a logarithmic scale). The blue lines represent the *p*-values obtained for each CNV threshold. The dashed horizontal line marks the unadjusted *p*-value threshold (*p*-value = 0.05). BH-adjusted *p*-values were not significant. (A) *TP53*, (B) *BRAF*, (C) *RB1*, (D) *MET*, (E) *MDM2*, and (F) *HSP90* at B2, and (G) *TP53*, (H) *BRAF*, (I) *RB1*, (J) *MET*, (K) *MDM2*, and (L) *HSP90* at B3.

genomic alterations support the biological relevance of these CNV patterns (Figure 2). The positive association of tumor size with progression is expected and aligns with established prognostic indicators in sarcoma (Figure 2). The observed correlation between treatment response and necrosis suggests that histologic tumor injury is a reliable marker of therapeutic efficacy, consistent with widely used grading systems such as the FNFCC and EORTC-STBSG score.[43,44] While the EORTC-STBSG score provides a valuable framework for assessing pathologic response in STS following neoadjuvant treatment, its prognostic role remains uncertain.[45,46] Significantly, linking these clinical features to evolving CNV patterns suggests that circulating CNV signatures may provide complementary information on tumor burden and response. The patterns observed across time points (B1–B6) may highlight dynamic and biologically meaningful relationships between CNVs in key cancer-related genes and clinical parameters in patients with STS (Figure 2).

The consistent and strong clustering of *TP53, RB1, MDM2, BRAF, MET,* and *HSP90* within B1–B4 (statistically significant positive correlations both between and within time points) suggests that early in the disease course or at the earliest sampling point, genomic instability affecting these pathways may be tightly coordinated (Figure 2). This interconnected CNV signature may reflect early tumor biology driven by alterations in cell-cycle control, proliferation pathways, and stress-response mechanisms.[21,22,38] Such early genomic synchrony has been described in aggressive sarcoma subtypes and may indicate a foundational genomic profile established before treatment initiation.[21]

As the disease progresses through B4–B6, the correlations between biomarkers became weaker and more heterogeneous, showing a weak correlation between B4 and B5 and a weak negative correlation between B5 and B6, with the exception noted in Figure 2. This may reflect tumor evolution, treatment pressure, or increasing intratumoral heterogeneity. The decrease in coherence of CNV patterns over time may align with the concept of genomic diversification during sarcoma progression.[47] Of particular interest is the persistent link between *TP53,*

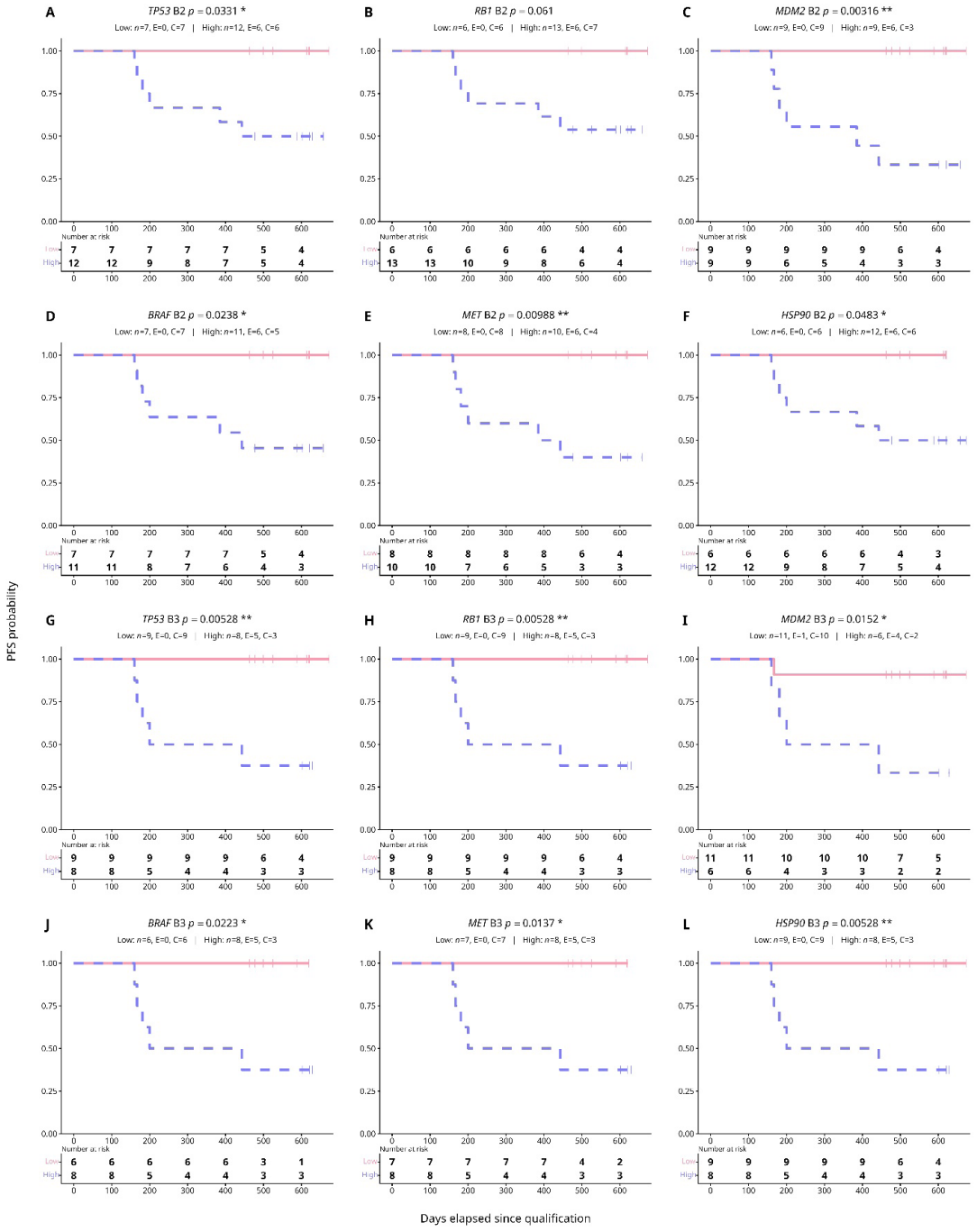


Figure 8. Progression-free survival (PFS) according to copy number variation (CNV) levels of cancer-related genes at B2 and B3. Kaplan–Meier curves illustrate PFS stratified by low versus high CNVs of *TP53, RB1, MDM2, BRAF, MET*, and *HSP90* measured at B2 and B3. Patients were dichotomized using gene-specific CNV thresholds: (A) B2_*TP53* (<16,535 vs. ≥16,535), (B) B2_*RB1* (<5,985 vs. ≥5,985), (C) B2_*MDM2* (<18,532 vs. ≥18,532), (D) B2_*BRAF* (<18,305 vs. ≥18,305), (E) B2_MET (<9,332 vs. ≥9,332), (F) B2_*HSP90* (<11,553 vs. ≥11,553), (G) B3_*TP53* (<8,075 vs. ≥8,075), (H) B3_*RB1* (<3,695 vs. ≥3,695), (I) B3_*MDM2* (<8852 vs. ≥8852), (J) B3_*BRAF* (<8,103 vs. ≥8,103), (K) B3_*MET* (<5,463 vs. ≥5,463), and (L) B3_*HSP90* (<7,028 vs. ≥7,028). Low-CNV groups are shown in pink (solid lines), and high-CNV groups in blue (dashed lines). Vertical tick marks indicate censored observations. For each group, *n* denotes the number of patients, E the number of progression events, and C the number of censored observations. The tables below each Kaplan–Meier curve show the number of patients at risk at the indicated time points; the number at risk represents patients who remain under observation and have neither experienced progression nor been censored immediately before that time point. *p* indicates the unadjusted *p*-value; after Benjamini–Hochberg correction for multiple testing, none of the associations remained statistically significant at the 0.05 threshold.

RB1, MDM2, MET, and *HSP90* across multiple time points (Figure 2). We hypothesize that coordinated genomic alterations among the analyzed biomarkers underlie sarcoma progression. Among them, tumor protein 53 (TP53) pathway alterations are key drivers of sarcoma biology, suggesting that CNV-based monitoring of *TP53* and its network partners may have predictive value. Recurrent correlations between *RB1* and *MDM2* across multiple time points potentially reflect shared regulatory mechanisms affecting cell-cycle control and genomic stability.[48] In parallel, the episodic yet notable correlations between *HSP90* and *MET* may be linked to cellular stress responses and receptor tyrosine kinase signaling pathways, which have been implicated in sarcoma aggressiveness and therapeutic resistance.[46]

In our study, *MDM2* CNV tended to be higher in non-responders in the unadjusted baseline analysis (Figure 4). Furthermore, *MDM2* CNV appeared to increase during therapy among patients who experienced disease progression (Figure 5). An increase was particularly notable following ChTh, with subtle differences seen between patients with and without progression (Figure 5). *MDM2* levels also showed a tendency to be higher in patients with disease progression compared to those without after RTh. Based on these findings, we hypothesize that coordinated genomic alterations among the analyzed biomarkers may contribute to, or be associated with, sarcoma progression; however, this relationship remains to be fully elucidated.

On the other hand, *TP53* levels increased in all patients after ChTh and continued to rise after RTh in patients who would experience progression, compared with those who would not, whereas they remained stable in those without progression (Figure 5). However, these results did not remain statistically significant after BH adjustment for multiple testing; therefore, they should be considered hypothesis-generating. Small cohort size and exploratory statistical framework preclude definitive conclusions.

We hypothesize that the CNV profile distinguishing responders from non-responders highlights the central role of the *TP53–MDM2–HSP90* axis in therapy resistance (Figure 4). *MDM2* CNVs in non-responders appeared to be among the most prominent genomic alterations (Figure 4), potentially contributing to functional suppression of TP53-driven apoptosis.[25,26] Our data suggest that *MDM2* CNVs may represent a key genomic alteration in non-responders (Figure 4), with notable enrichment in molecular progression subgroups B2 and B3 (Figure 4). This subgroup-specific increase in *MDM2* CNVs may indicate a recurrent genomic mechanism that could contribute to functional suppression of TP53-mediated apoptosis, a pathway often implicated in sarcoma progression and treatment resistance.[25,26] *MDM2* CNV levels differed between patients in various progression groups at time points B2 and B3, with a tendency toward higher levels in those who progressed after treatment (Figure 5). These findings imply that *MDM2* CNV may be associated with poorer treatment response.[49,50] However, *BRAF* CNV did not differ significantly between patients with and without sarcoma progression, suggesting that it is not associated with progression in this cohort. B2 and B3 were selected for further exploratory analyses because these time points exhibited the greatest separation in CNV profiles between patients with and without subsequent disease progression. Although treatment may influence circulating CNV levels, these measurements may also reflect early molecular responses to therapy and therefore warrant further investigation in larger cohorts. The inverse correlations observed between CNV measurements at B2/B3 and later follow-up time points (B5/B6) may reflect dynamic changes in ctDNA during treatment and subsequent recovery. These temporal changes could be associated with treatment-induced reduction in tumor burden, differential clonal dynamics, or biological heterogeneity among patients. Nevertheless, because of the exploratory nature of this study and the limited cohort size, these findings should be interpreted cautiously and require validation in larger longitudinal cohorts.

The observation that *MDM2* alterations cluster within defined molecular groups suggests that deregulation of the TP53 axis may not be uniformly distributed across STS, but could instead characterize specific biological subsets. These findings are consistent with reports from other groups demonstrating the importance of MDM2 as a circulating and prognostic biomarker.[14,23,24,38] Prior studies showed that *MDM2* isolated from extracellular vesicles is elevated in patients with well-differentiated and dedifferentiated liposarcoma before surgery and decreases after tumor removal, while postoperative increases signal recurrent or persistent disease.[23] Similarly, Bill *et al.*[24] reported that increased *MDM2* amplification and mRNA expression in dedifferentiated liposarcoma correlate with shorter recurrence-free and overall survival. The expression levels of *TP53* and *MDM2* could serve as important prognostic indicators for hepatocellular carcinoma.[27] Early diagnostic methods for hepatocellular carcinoma are limited, but alterations in the MDM2–p53 pathway may offer a more effective diagnostic approach, thereby improving surgical outcomes. Additionally, *MDM2* is linked to various solid tumors, including non-small cell lung and colorectal cancers, with overexpression associated with poor prognosis and the risk of hyperprogressive disease.[27] Together, these observations support a central role for *MDM2* dysregulation in sarcoma biology and highlight

its potential as a biomarker for disease monitoring. Analyzing CNVs may be vital for sarcoma diagnosis, as *MDM2* amplification affects tumor classification and treatment.[51-55] The MDM2–p53 pathway is vital for tumor suppression, and its dysregulation is linked to increased cell proliferation, survival, and ChTh resistance.[25,26] The results indicate that alterations in *MDM2* CNV may be associated with a poorer treatment response, underscoring the potential of *MDM2* as a candidate therapeutic target and biomarker. Nevertheless, these observations remain exploratory because of the limited cohort size and the lack of matched tumor genomic profiling. Consequently, the biological relationship between circulating *MDM2* CNV and tumor genomic alterations could not be established in the present study.

Detecting *MDM2* CNV in blood samples may serve as a minimally invasive method for monitoring disease. Targeting *MDM2*, whether alone or in combination with other therapies, should be further explored to improve sarcoma treatment outcomes.[48,55]

The findings from time points B2 and B3 consistently demonstrate that elevated CNV levels across multiple cancer-related genes were associated with poorer PFS, suggesting that increased genomic instability during these phases reflects a more aggressive disease phenotype (Figures 6–8). The robust associations observed for *MDM2* and *MET* at B2 (Figures 2 and 5), together with the significant correlations identified for *TP53, RB1, BRAF, MET,* and *HSP90* at B3 (Figure 2), indicate coordinated dysregulation of several oncogenic pathways involved in cell-cycle regulation, proliferation, and cellular stress responses. PFS curves for groups with high and low *MDM2* did not reach statistically significant differences at B3 (Figures 6–8), but the trend toward poorer PFS aligns with its known role in suppressing TP53 signaling.[28] Collectively, these results highlight CNV profiling at intermediate time points (B2 and B3) as a promising prognostic approach for identifying patients at increased risk of early progression and informing risk-adapted monitoring or therapeutic strategies.

Concurrently, increased CNVs in *HSP90* (Figure 4), a molecular chaperone that stabilizes multiple oncogenic client proteins, may further enhance resistance mechanisms by maintaining the activity of proliferative and anti-apoptotic signaling pathways.[34] The reduction in *RB1* CNV in non-responders (Figure 4) suggests that loss of cell-cycle checkpoint control is an additional contributor to treatment failure.[35] The retinoblastoma (RB1) protein is a key regulator of the cell cycle, particularly at the G1-to-S transition. By binding to E2F transcription factors, RB1 suppresses the expression of genes required for DNA synthesis, thereby maintaining controlled cell proliferation and promoting differentiation. Loss or inactivation of *RB1* disrupts this checkpoint, leading to uncontrolled cell growth and tumor development.[35] An alternative hypothesis is that CNV-dependent deregulation of tumor suppressor and stress-response pathways, rather than amplification of the mitogen-activated protein kinase (MAPK) pathway, drives therapy resistance. Our findings suggest that changes in *MDM2* CNV are associated with poorer treatment response in sarcoma patients, highlighting *MDM2* as a relevant molecular target. This indicates that *MDM2* may be considered both a prognostic biomarker and a promising therapeutic target, particularly in *MDM2*-dysregulated sarcomas. Further clinical studies should explore targeting *MDM2*, either alone or in combination with other therapies, to improve treatment efficacy and patient outcomes. Our findings indicate that all biomarkers at time point B1 form a highly interconnected cluster (Figure 2), with significant correlations observed between nearly every pair of markers. The findings for B5 suggest partial internal coherence within the time point. Overall, these findings suggest that elevated plasma levels of the analyzed markers are associated with disease progression (Figures 6–8).

Overall, the correlation structure observed across B1–B6 supports a model in which sarcoma CNVs form tightly connected genomic networks early in disease but may evolve toward greater diversity over time. These findings highlight the potential utility of CNV profiling as a dynamic biomarker strategy that reflects both tumor biology and therapeutic response. As no circulating genomic biomarkers have been validated for sarcoma[1], this work may provide foundational evidence to guide further exploration of CNV-based LB approaches in this rare and heterogeneous cancer group. In our study, since tumor tissue was not analyzed in parallel, we cannot determine whether the plasma-derived signals exclusively reflect tumor genomic alterations or are partially influenced by total cfDNA release, treatment-related tissue injury, inflammatory responses, or other non-tumor sources of cfDNA.

Our study has several limitations. The study includes a small cohort of 19 participants with diverse subtypes of STS and some variation in treatment exposure (e.g., hyperthermia administration and slight differences in intervals between consecutive treatment stages), which may limit the generalizability and statistical power of the findings. Consistent with this limitation, several associations observed in the unadjusted analyses did not remain statistically significant after BH correction for multiple testing, highlighting the exploratory nature of

the study. Variations in ChTh and RTh regimens among patients may have influenced CNV profiles and response patterns, leading to unmanageable confounding effects. The restricted biomarker panel includes six key CNV biomarkers: *TP53, MDM2, RB1, BRAF, MET,* and *HSP90*. While these genes are candidate biomarkers for STS, this panel does not capture the full genomic complexity of STS, as other genetic alterations may also influence disease progression and treatment resistance. In the absence of tissue–plasma concordance analysis, matched tumor tissue was not analyzed alongside plasma samples, thereby preventing a direct assessment of concordance between circulating CNVs and tumor genomic alterations; however, this was beyond the scope of the present study. Other circulating biomarkers, such as point mutations, gene fusions, methylation patterns, and exosome-associated nucleic acids, were not assessed and may provide complementary prognostic information; however, this was beyond the scope of the present study. PFS analyses were exploratory, and the multivariable modeling, which adjusted for established clinical prognostic factors, was limited. The interpretation of biomarker trajectories was limited by incomplete sampling in some patients. Missing blood samples affected our understanding of changes and may have concealed significant alterations. Future studies should use more frequent and standardized sampling to better assess biomarker dynamics during treatment and disease progression. Although the ddPCR Copy Number Assays normalize target copy number to a stable reference locus and plasma-normalized values (copies/mL plasma) were subsequently calculated, part of the observed correlations among biomarkers may still reflect variation in overall cfDNA abundance or pre-analytical sample characteristics rather than exclusively coordinated tumor genomic alterations. The threshold optimization procedure was exploratory and intended for hypothesis generation; therefore, the identified cut-off values should not be considered clinically meaningful, and independent external validation is required before any clinical application. We also note that none of the threshold-based associations remained statistically significant after BH correction, further emphasizing the exploratory nature of these analyses.

5. Conclusion

Longitudinal CNV profiling using LB may reveal dynamic genomic alterations in STS and may provide additional information on tumor evolution during treatment. We hypothesize that deregulation of the TP53–MDM2–RB1 axis and stress-response pathways contributes to therapy resistance and disease progression; however, this remains exploratory. In particular, *MDM2* CNV may represent a promising prognostic and potentially therapeutic biomarker candidate. However, its prognostic and therapeutic relevance requires validation in larger prospective cohorts. These preliminary findings provide foundational evidence supporting CNV-based LB strategies for risk stratification, treatment monitoring, and personalized management in STS. The variability in biomarker responses among patients with progressing disease suggests that CNV-based biomarkers should not be used alone as predictors. They may be more effective when combined with clinical and radiological data, highlighting the need for multi-marker models in high-risk STS.

Acknowledgments

None.

Funding

This research was funded by NCN (2023/49/B/NZ5/03294) and POB Biotechnology and Biomedical Engineering of Warsaw University of Technology within the Excellence Initiative: Research University (IDUB) programme (LIDER POB BIB-2 nr CPR-IDUB/73/Z01/POB4/2024 [22.03.2024]).

Conflict of interest

The authors declare they have no competing interests.

Author contributions

Conceptualization: Aneta Borkowska, Piotr Rutkowski, Monika Staniszewska, Teresa Szczepińska

Formal analysis: Teresa Szczepińska, Monika Staniszewska, Wiktoria Trynkos, Michał Sitek

Investigation: Aneta Borkowska, Piotr Rutkowski, Monika Staniszewska, Teresa Szczepińska, Wiktoria Trynkos, Michał Sitek, Ewelina Holm Bidstrup, Izabela Ziuzia-Graczyk, Deepak Kala, Anna Staniszewska

Methodology: Monika Staniszewska, Teresa Szczepińska, Aneta Borkowska, Łukasz Kuryk, Piotr Rutkowski

Writing–original draft: Aneta Borkowska, Monika Staniszewska, Teresa Szczepińska, Anna Staniszewska, Deepak Kala

Writing–review & editing: Lukasz Kuryk, Piotr Rutkowski, Monika Staniszewska, Aneta Borkowska, Teresa Szczepińska

Ethics approval and consent to participate

The study was approved by the Ethics Committee at NIO (protocol code No. 53/2024). Written informed consent for participation was obtained from all participants.

Consent for publication

Written informed consent for publication was obtained from all participants.

Availability of data

All data generated or analyzed during this study are included in the manuscript and the Supplementary File. The Supplementary Dataset contains the patient-level data required to reproduce the principal statistical analyses presented in the manuscript. Any additional information not included in the Supplementary File or Supplementary Dataset is available from the corresponding author upon reasonable request, subject to applicable ethical and data protection regulations.

Further disclosure

This work has been presented as a poster, titled "Longitudinal Copy Number Variation in Sarcoma Patients Predicts Therapeutic Response and Disease Progression," at ctDNA Symposium 2026, Circulating Tumor DNA in Cancer: From Biology to Clinical Practice and Beyond, May 21–22, 2026, Aarhus, Denmark.

A preprint version of this manuscript has been deposited on Research Square (doi:10.21203/rs.3.rs-9442446/v1).

References

1. Williams TP, Grignol VP. Circulating biomarkers in sarcoma. *Curr Oncol Rep*. 2025;27(8):1013-1018.

   doi: 10.1007/s11912-025-01692-0

2. Clark MA, Fisher C, Judson I, Thomas JM. Soft-tissue sarcomas in adults. *N Engl J Med*. 2005;353(7):701-711.

   doi: 10.1056/NEJMra041866

3. Califf RM. Biomarker definitions and their applications. *Exp Biol Med (Maywood)*. 2018;243(3):213-221.

   doi: 10.1177/1535370217750088

4. Sharma SR, Paonessa NE, Casadei L, Costas De Faria F, Pollock RE, Grignol V. Clinical biomarkers in soft tissue sarcoma: a comprehensive review of current soft tissue sarcoma biomarkers. *J Surg Oncol*. 2022;125(2):239-245.

   doi: 10.1002/jso.26680

5. Grasso D, Marzocchi B, Scoccianti G, *et al*. Untargeted metabolomics and liquid biopsy investigation of circulating biomarkers in soft tissue sarcoma. *Cancers (Basel)*. 2025;17(3):553.

   doi: 10.3390/cancers17030553

6. Li X, Seebacher NA, Hornicek FJ, Xiao T, Duan Z. Application of liquid biopsy in bone and soft tissue sarcomas: present and future. *Cancer Lett*. 2018;439:66-77.

   doi: 10.1016/j.canlet.2018.09.012

7. Bettegowda C, Sausen M, Leary RJ, *et al*. Detection of circulating tumor DNA in early- and late-stage human malignancies. *Sci Transl Med*. 2014;6(224):224ra24.

   doi: 10.1126/scitranslmed.3007094

8. Cohen JD, Li L, Wang Y, *et al*. Detection and localization of surgically resectable cancers with a multi-analyte blood test. *Science*. 2018;359(6378):926-930.

   doi: 10.1126/science.aar3247

9. Snow A, Chen D, Lang JE. The current status of the clinical utility of liquid biopsies in cancer. *Expert Rev Mol Diagn*. 2019;19(11):1031-1041.

   doi: 10.1080/14737159.2019.1664290

10. Aiyer S, Kim TH, Collier K, *et al*. Unlocking the potential of ctDNA in sarcomas: a review of recent advances. *Cancers (Basel)*. 2025;17(6):1040.

    doi: 10.3390/cancers17061040

11. Coombs CC, Dickherber T, Crompton BD. Chasing ctDNA in patients with sarcoma. *Am Soc Clin Oncol Educ Book*. 2020;40:e351-e360.

    doi: 10.1200/EDBK_280749

12. Przybyl J, Chabon JJ, Spans L, *et al*. Combination approach for detecting different types of alterations in circulating tumor DNA in leiomyosarcoma. *Clin Cancer Res*. 2018;24(11):2688-2699.

    doi: 10.1158/1078-0432.CCR-17-3704

13. Braig D, Becherer C, Bickert C, *et al*. Genotyping of circulating cell-free DNA enables noninvasive tumor detection in myxoid liposarcomas. *Int J Cancer*. 2019;145(4):1148-1161.

    doi: 10.1002/ijc.32216

14. Cocucci E, Racchetti G, Meldolesi J. Shedding microvesicles: artefacts no more. *Trends Cell Biol*. 2009;19(2):43-51.

    doi: 10.1016/j.tcb.2008.11.003

15. Capdevila P, Carrasco C, Diaz-Beveridge R. Risk stratification in soft-tissue sarcoma using Sarculator: a single-center experience. *ESMO Rare Cancers*. 2025;4:100114.

    doi: 10.1016/j.esmorc.2025.100114

16. Amin MB, Edge SB, Greene FL, *et al*, eds. *AJCC Cancer Staging Manual*. 8th ed. Springer; 2017.

17. Edge SB, Byrd DR, Compton CC, Fritz AG, Greene FL, Trotti A, eds. *AJCC Cancer Staging Manual*. 7th ed. Springer; 2010.

18. Nathan H, Raut CP, Thornton K, *et al*. Predictors of survival after resection of retroperitoneal sarcoma. *Ann Surg*. 2009;250(6):970-976.

    doi: 10.1097/sla.0b013e3181b25183

19. Massarweh NN, Dickson PV, Anaya DA. Soft tissue

sarcomas: staging principles and prognostic nomograms. *J Surg Oncol*. 2015;111(5):532-539.

doi: 10.1002/jso.23851

20. ESMO/European Sarcoma Network Working Group. Soft tissue and visceral sarcomas: ESMO Clinical Practice Guidelines for diagnosis, treatment and follow-up. *Ann Oncol*. 2014;25(suppl 3):iii102-iii112.

doi: 10.1093/annonc/mdu254

21. Callegaro D, Miceli R, Mariani L, Raut CP, Gronchi A. Soft tissue sarcoma nomograms and their incorporation into practice. *Cancer*. 2017;123(15):2802-2820.

doi: 10.1002/cncr.30721

22. Chibon F, Lagarde P, Salas S, *et al*. Validated prediction of clinical outcome in sarcomas and multiple types of cancer on the basis of a gene expression signature related to genome complexity. *Nat Med*. 2010;16(7):781-787.

doi: 10.1038/nm.2174

23. Casadei L, Calore F, Braggio DA, *et al*. MDM2 derived from dedifferentiated liposarcoma extracellular vesicles induces MMP2 production from preadipocytes. *Cancer Res*. 2019;79(19):4911-4922.

doi: 10.1158/0008-5472.CAN-19-0203

24. Bill KLJ, Seligson ND, Hays JL, *et al*. Degree of MDM2 amplification affects clinical outcomes in dedifferentiated liposarcoma. *Oncologist*. 2019;24(7):989-996.

doi: 10.1634/theoncologist.2019-0047

25. Brooks CL, Gu W. p53 ubiquitination: Mdm2 and beyond. *Mol Cell*. 2006;21(3):307-315.

doi: 10.1016/j.molcel.2006.01.020

26. Manfredi JJ. Mdm2 and MdmX: partners in p53 destruction. *Cancer Res*. 2021;81(7):1633-1634.

doi: 10.1158/0008-5472.CAN-21-0145

27. Yao Y, Zhang Q, Li Z, Zhang H. MDM2: current research status and prospects of tumor treatment. *Cancer Cell Int*. 2024;24(1):170.

doi: 10.1186/s12935-024-03356-8

28. Fontecha MB, Del Rosario Anadón M, Lahitou IMM, *et al*. Exploring the significance of MDM2 gene promoter variants in chronic myeloid leukemia. *Leuk Res*. 2025;149:107644.

doi: 10.1016/j.leukres.2025.107644

29. Momand J, Jung D, Wilczynski S, Niland J. The MDM2 gene amplification database. *Nucleic Acids Res*. 1998;26(15):3453-3459.

doi: 10.1093/nar/26.15.3453

30. Oliner JD, Saiki AY, Caenepeel S. The role of MDM2 amplification and overexpression in tumorigenesis. *Cold Spring Harb Perspect Med*. 2016;6(6):a026336.

doi: 10.1101/cshperspect.a026336

31. Oliner JD, Kinzler KW, Meltzer PS, George DL, Vogelstein B. Amplification of a gene encoding a p53-associated protein in human sarcomas. *Nature*. 1992;358(6381):80-83.

doi: 10.1038/358080a0

32. Su Q, Hou J, Du X, *et al*. The role and research progress of the MET signalling pathway in targeted therapy for osteosarcoma. *Oncol Rev*. 2025;19:1615111.

doi: 10.3389/or.2025.1615111

33. Chen N, Zhang Q, Sun L, *et al*. Comprehensive study of gene fusions in sarcomas. *Invest New Drugs*. 2025;43(1):3-17.

doi: 10.1007/s10637-024-01486-4

34. Liu Y, Li C, Liu H, Tan S. Combination therapy involving HSP90 inhibitors for combating cancer: an overview of clinical and preclinical progress. *Arch Pharm Res*. 2024;47(5):442-464.

doi: 10.1007/s12272-024-01494-1

35. Shim BY, Yoo J, Lee YS, Hong YS, Kim HK, Kang JH. Prognostic role of Rb, p16, cyclin D1 proteins in soft tissue sarcomas. *Cancer Res Treat*. 2010;42(3):144-150.

doi: 10.4143/crt.2010.42.3.144

36. Yang Z, Carrio-Cordo P, Baudis M. Copy number variation heterogeneity reveals biological inconsistency in hierarchical cancer classifications. *Mol Cytogenet*. 2024;17(1):26.

doi: 10.1186/s13039-024-00692-2

37. Lei C, Zang H, Zhang H, *et al*. RNA-based next-generation sequencing strategy for screening MDM2-amplified sarcomas. *Sci Rep*. 2026;16(1):16402.

doi: 10.1038/s41598-026-46618-3

38. Calore F, Casadei L, Sarchet PD, *et al*. Extracellular vesicle-MDM2-DNA as a potential liquid biopsy biomarker for disease identification in retroperitoneal liposarcoma. *Ann Surg*. 2025;281(6):1048-1054.

doi: 10.1097/SLA.0000000000006345

39. Huber C, Zinserling J, Benda N, Vetter T, Rueckbeil M. Methodological insights on biomarker-based patient selection: a review of scientific advice procedures at the European Medicines Agency. *Clin Pharmacol Ther*. 2025;117(5):1226-1235.

doi: 10.1002/cpt.3558

40. Wang Y, Fujiwara T, Kurozumi T, *et al*. Advances in liquid biopsy for bone and soft-tissue sarcomas. *Int J Clin Oncol*. 2025;30(9):1722-1733.

doi: 10.1007/s10147-025-02813-2

41. Gronchi A, Miah AB, Dei Tos AP, *et al*. Soft tissue and visceral sarcomas: ESMO-EURACAN-GENTURIS Clinical Practice Guidelines for diagnosis, treatment and follow-up. *Ann Oncol*. 2021;32(11):1348-1365.

doi: 10.1016/j.annonc.2021.07.006

42. Casali PG, Abecassis N, Aro HT, *et al*. Soft tissue and visceral sarcomas: ESMO-EURACAN Clinical Practice Guidelines for diagnosis, treatment and follow-up. *Ann Oncol*. 2018;29(suppl 4):iv51-iv67.

doi: 10.1093/annonc/mdy096

43. Spałek MJ, Koseła-Paterczyk H, Borkowska A, *et al*. Combined preoperative hypofractionated radiotherapy with doxorubicin-ifosfamide chemotherapy in marginally resectable soft tissue sarcomas: results of a phase 2 clinical trial. *Int J Radiat Oncol Biol Phys*. 2021;110(4):1053-1063.

doi: 10.1016/j.ijrobp.2021.02.019

44. Stergioula A, Kormas T, Kokkali S, *et al*. What is the prognostic value of the pathologic response after neoadjuvant radiotherapy in soft tissue sarcoma? An institutional study using the EORTC-STBSG response score. *Cancers (Basel)*. 2024;16(20):3449.

doi: 10.3390/cancers16203449

45. Spałek MJ, Borkowska AM, Telejko M, *et al*. The feasibility study of hypofractionated radiotherapy with regional hyperthermia in soft tissue sarcomas. *Cancers (Basel)*. 2021;13(6):1332.

doi: 10.3390/cancers13061332

46. Laurini JA. *Protocol for the Examination of Specimens From Patients With Soft Tissue Tumors*. College of American Pathologists; June 2021. Accessed October 13, 2026. https://www.cap.org/wp-content/uploads/protocols/Soft.Tissue.Bx_4.1.0.0.REL_CAPCP_R.pdf?download=true

47. Wardelmann E, Haas RL, Bovée JV, *et al*. Evaluation of response after neoadjuvant treatment in soft tissue sarcomas; the European Organization for Research and Treatment of Cancer-Soft Tissue and Bone Sarcoma Group (EORTC-STBSG) recommendations for pathological examination and reporting. *Eur J Cancer*. 2016;53:84-95.

doi: 10.1016/j.ejca.2015.09.021

48. Schaefer IM, Hornick JL, Barysauskas CM, *et al*. Histologic appearance after preoperative radiation therapy for soft tissue sarcoma: assessment of the European Organization for Research and Treatment of Cancer-Soft Tissue and Bone Sarcoma Group response score. *Int J Radiat Oncol Biol Phys*. 2017;98(2):375-383.

doi: 10.1016/j.ijrobp.2017.02.087

49. Schmiester M, Freytag A, Gillissen B, *et al*. Genomic evolution of high-risk soft tissue sarcomas under thermo- and chemotherapeutic selection pressure. *Int J Hyperthermia*. 2025;42(1):2573753.

doi: 10.1080/02656736.2025.2573753

50. Hernandez-Monge J, Martínez-Sánchez M, Rousset-Roman A, Medina-Medina I, Olivares-Illana V. MDM2 regulates RB levels during genotoxic stress. *EMBO Rep*. 2021;22(1):e50615.

doi: 10.15252/embr.202050615

51. Wei H, Zhang Y, Jia Y, *et al*. Heat shock protein 90: biological functions, diseases, and therapeutic targets. *MedComm (2020)*. 2024;5(2):e470.

doi: 10.1002/mco2.470

52. Zhang J, He P. In silico and in vitro assessment of TP53, ATM, RAD51, and BAX genes in gastric cancer and their contribution to radiotherapy resistance. *Hereditas*. 2025;162(1):125.

doi: 10.1186/s41065-025-00496-3

53. Vargas R, Petty A, Lindner DJ, *et al*. Synergistic effect of MDM2 inhibitors and radiotherapy in endometrial cancer. *NPJ Precis Oncol*. 2025;9(1):290.

doi: 10.1038/s41698-025-01063-9

54. Kim YJ, Kim M, Park HK, *et al*. Co-expression of MDM2 and CDK4 in transformed human mesenchymal stem cells causes high-grade sarcoma with a dedifferentiated liposarcoma-like morphology. *Lab Invest*. 2019;99(9):1309-1320.

doi: 10.1038/s41374-019-0263-4

55. Steele CD, Pillay N. The genomics of undifferentiated sarcoma of soft tissue: progress, challenges and opportunities. *Semin Cancer Biol*. 2020;61:42-55.

doi: 10.1016/j.semcancer.2019.11.009